CAPTURING HUMAN HAND KINEMATICS

FOR OBJECT GRASPING AND MANIPULATION

A Thesis

by

SHRAMANA GHOSH

Submitted to the Office of Graduate Studies of
Texas A&M University
in partial fulfillment of the requirements for the degree of

MASTER OF SCIENCE

Approved by:

Chair of Committee,   Amarnath Banerjee
Co-Chair of Committee,   Nina P. Robson
Committee Member,   John J. Buchanan
Head of Department,   Cesar O. Malave

May 2013

Major Subject: Industrial Engineering

CDUVTCEV

The aim of this thesis is to create a low-cost sensor equipped glove using commercially available components that can be used to obtain position, velocity and acceleration data for individual fingers of a hand within an optical motion capture environment. Tracking the full degrees of freedoms of the hand and finger motions without any hindrances is a challenging task in optical motion capture measurements. Attaching markers on every finger and hand joint makes motion capture systems troublesome due to practical problems such as blind spots and/or obtaining higher derivative motion constraints, such as velocities and accelerations. To alleviate this, we propose a method to capture the hand and finger kinematics with a reduced set of optical markers. Additionally inertial sensors are attached to the fingertips to obtain linear acceleration measurements. For optimal velocity estimation, a Kinematic Kalman Filter (KKF) is implemented and its result is compared to the time derivative of the Motion Capture System measurement. The higher derivative specifications are related to contact and curvature constraints between the fingers and the grasped object and are later used in formulating the synthesis task for the design of robotic fingers and hands. A preliminary prototype device has been developed to obtain position, velocity and acceleration information of each fingertip by incorporating multiple accelerometers into the basic design of reduced marker set.

To my parents

ACKNOWLEDGEMENTS

First of all I would like to thank Dr. Nina Robson for accepting me as a master's student. Her patient guidance, help and encouragement has been invaluable to me over the last two years. I would also like to thank Dr. Amarnath Banerjee for serving as the chair of my committee, and for his ready help and guidance at every stage. I want to thank Dr. John Buchanan, who kindly agreed to complete my committee. This work would not have been possible without the constant guidance and contributions of Hyosang Moon. Additionally I would also like to thank my friends and colleagues and the department faculty and staff for making my time at Texas A&M University a great experience. Finally, thanks to my mother and father for their unfailing support.

PQO GPENCVWTG

DOF	Degrees of Freedom
DIP	Distal Interphalangeal
IK	Inverse Kinematics
IMU	Inertial Measurement Unit
IP	Interphalangeal
IR	Infrared
KKF	Kinematic Kalman Filter
MCP	Metacarpophalageal
PIP	Proximal Interphalangeal
RMSE	Root Mean Squared Error
RR	Kinematic Chain With Two Revolute Joints
RRR	Kinematic Chain With Three Revolute Joints

TABLE OF CONTENTS

LIST OF FIGURES

LIST OF TABLES

1. INTRODUCTION

Tracking the motion of human hand is an important area of research with applications in animation, gesture recognition, robotic control, teleoperation, sign language processing and human-computer interaction. Amongst these applications the study of biomechanics of human hand motion is particularly important for development of multi-fingered robotic devices that can carry out tasks such as grasping and object manipulation.

1.1 Human Hand Kinematics

The human hand is an incredibly complex structure, and the most dexterous and versatile biomechanical component of the human body with a large number of controllable degrees of freedoms (DOFs). The different types of skeletal joints comprising the human hand can be seen in Fig. 1. This highly articulated structure of the hand is the basis of its dexterity. On the other hand, the existence of these multiple DOFs makes accurate modeling of the human hand difficult. Numerous models describing the biomechanics of the hand and using a variety of simplifications have been reported in the literature. Bullock et al. [1] present a review of some of the models used in literature and examine the trade-offs associated with implementing simplified kinematic models which provide simpler analytical solutions, ease of implementation, or speed up computation for real time applications.
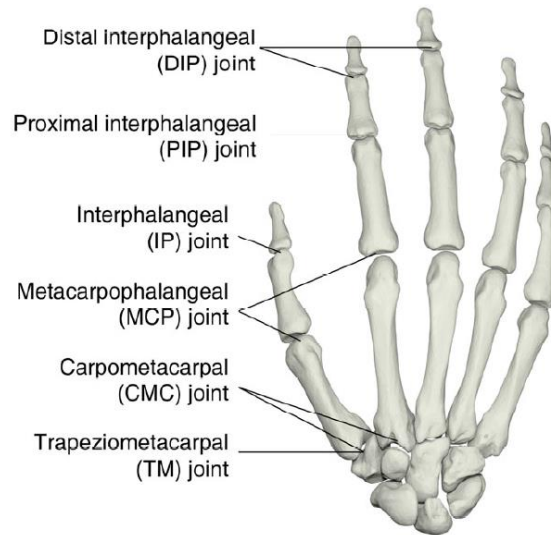
Figure 1. Skeletal Model of Human Hand (from [1])

Of these, one of the most commonly used kinematic model of human hand in literature is the 27 DOF model (see Fig. 2) [2, 3]. In this model, each of the four fingers has four DOFs. The distal interphalangeal (DIP) joint and proximal interphalangeal (PIP) joint each have one DOF for flexion-extension and are treated as revolute joints. The metacarpophalangeal (MCP) joint has two DOFs due to flexion-extension and adduction-abduction and is modeled as a universal joint. The thumb has a different structure from the other four fingers: it has five degrees of freedom, one for the interphalangeal (IP) joint (flexion-extension), and two each for the thumb MCP and trapeziometacarpal (TM) joints, due to flexion-extension and adduction-abduction. The fingers together have 21DOF. The remaining 6 degrees of freedom are from the rotational and translational motion of the wrist. These 6 parameters can ignored when

2

the focus is only on the estimation of the local finger motions rather than the global motion.
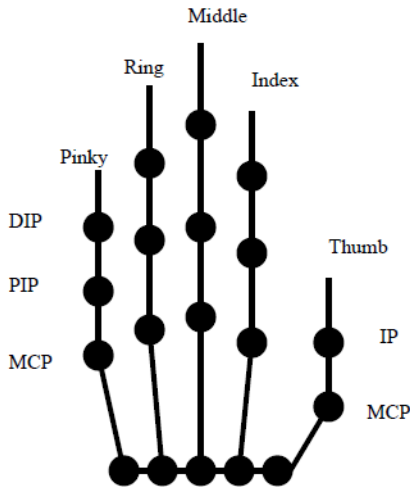
Figure 2. 27 DOF Simplified Kinematic Model of Human Hand (from [3])

This kinematic hand model assumes that the joints are all ideally revolute, universal or spherical. This simplifies the analysis of the model, and Bullock *et al*. [1] argue that the success of simplified hand models for robotic and grasping tasks suggest that this assumptions may not be considered problematic in this domain.

1.2 Hand Motion Tracking

Usually described with more than twenty Degrees of Freedom (DOFs), the human hand is a highly articulated object. While grasp formation and manipulation by the fingers require coordination of multiple DOFs, the hand has many more DOFs than are required to form a stable grasp. Thus the task has redundancies at many levels,

allowing many possibilities for the selection of grasp points, the orientation and posture of the hand, the forces to be applied at each fingertip and the impedance properties of the hand [4]. Despite this inherent complexity, humans perform object manipulation nearly effortlessly. Due to this, identification of human natural behavior during hand motions (e.g. grasping and manipulating a hand-held object) from experimental data can inspire better ideas in both design and control of multi-fingered robotic devices.

One of the most widely used methods to study the motion of human hands is optical motion capture using either retro-reflective or light emitting markers attached on specific points on the hand [5]. Optically tracking human hand motion is a complex problem due to the large number of DOFs packed in a relatively small space. Problems like blind spots and misidentification of features make motion capture and subsequent reconstruction difficult. Some of these problems can be alleviated by adopting a reduced marker set to capture the motion of the hand as well as by using non-optical sensors. For this purpose, we propose that optical motion capture be supplemented with inertial measurements (e.g. linear accelerations) from well-selected points and using the geometries of finger linkages to reduce the number of required measurement sites compare to the conventional approach.

Given standard descriptions of kinematics and link geometries, Cobos, *et al*. [6] present a treatment showing linkage parameter estimation and joint parameter calculations for a 24 DOF model. The approach of determining the joint angle trajectories, given a measured posture falls in the class of Inverse Kinematics (IK).

However, the complex structure of the hand, with its many natural constraints calls for an integrated forward and inverse kinematics approach [5].

1.3 Research Goals

The aim of this thesis is to develop a low-cost glove-based device that can provide information about position and orientation of the fingertips, linear and angular velocities and accelerations as well as joint angles of the fingers by utilizing infrared (IR) markers and inertial sensors. This information is then used for the synthesis of a mechanical linkage, according to a novel technique introduced by Robson, *et al.* [8-11]. This technique utilizes second order kinematic task specifications, related to the curvature of the body to be grasped and manipulated. Planar and spatial kinematic chains or fingers are then synthesized, such that they do not violate normal direction and curvature constraints imposed by contact of the fingers with an object. Finally, this is used to formulate and solve the synthesis equations for the chain/finger.

2. EXPECTED CONTRIBUTIONS

1. The prototype of a low-cost sensor based data glove is fabricated. This prototype uses commercially available components to capture information regarding all kinematic parameters of the hand, and provides position, velocity and acceleration specifications for fingertips. The glove incorporates inertial sensors, as well as a reduced optical marker set, and is used for enhancing the kinematic data obtained from commercially available motion capture systems. The glove is used for object grasping and manipulation studies, as well as for defining the position and higher derivative task specifications used in the geometric design of multi-fingered robotic hands. In this design synthesis, the accuracy of the kinematic measurements is critical to determine how well the designed linkage follows the original human motion.

2. A method that integrates the glove within a motion capture system environment is proposed and tested, with the main goal of reducing the error/noise in the higher order motion constraints.

3. A reduced marker set method/protocol, used for capturing the complete hand kinematics is developed and reported. The method calculates each joint angle assessed through inverse kinematics and then estimates the positions of every marker site from the forward kinematics of the modeled structure. In preliminary experiments, results of the proposed method and existing conventional methods

were compared and the difference was less than 2°. Relative skin movements were identified as the major source of error.

4. A comparison between the accuracy of the linear acceleration data obtained from the developed sensor-based data glove device and the data obtained from a Vicon motion capture system is presented. Possible causes for observed deviations between the two systems are explored.

5. Preliminary studies on the application of the developed sensor-glove device for the design of mechanical fingers for contact and curvature task constraints are presented.

3. LITERATURE REVIEW

3.1 Vision Based Techniques for Tracking Hand Kinematics

Tracking the motion of a human can be accomplished by using various methods based on mechanical, optical magnetic and inertial technologies. While methods for tracking human gait have been well developed, the use similar techniques for tracking the motion of the hands is complicated by many unique issues associated with it. Some of the commonly used methods for tracking and studying the kinematics of human hand motion are optical motion capture [5], instrumented data gloves [12] and vision-based tracking systems [13]. Of these the most widely used method is optical motion capture method, which utilizes a number of markers (either retro-reflective or light emitting) attached on the specific points on the hand and captures the 3D marker position with respect to pre-defined global coordinates with an array of overlapping cameras. The human hand motions can be acquired as numeric 3D position values of these specific points on the hand (e.g. every tip and joint of each finger) during motions. Instrumented gloves will be discussed in the next sub-section.

While optical motion capture is one of the most accurate methods available presently, capturing the full kinematics of a hand and fingers is a very challenging task due to the problems described in the following discussion. The primary complexity arises from the large number of degrees of freedom (DOFs) of the human hand packed in a relatively small space compared to any other section of the human body. Thus, most of the hand motion studies that employ video measurement systems focus on analyses of

single finger postures or motions, fingertip traces, joint flexion-extension and finger coordination patterns [14].

In case of multi-finger motion capture, even though the size of reflective markers is small, attaching a correspondingly large number of markers on the hand induces practical problems such as blind spots, i.e. reflections from some of the markers can be blocked from reaching the cameras either by other markers or other sections of the hand. In addition, geometrical similarities between fingers, which are located close to each other, can lead to misidentification of markers even in case of multiple cameras observing the scene [15]. One solution for the problem of multiple blind spots and marker misidentification is to reduce the number of markers that need to be tracked, via reduced marker protocols [7,16].To derive reduced marker protocols, Miyata, *et al.* [7] suggest that the following conditions must be satisfied:

1. Each joint should be modeled with adequate but not useless DOFs to reconstruct the necessary characteristics of the captured motion, and

2. Fingertip positions of the captured data should be reconstructed with an accuracy of few millimeters.

The first condition is to be satisfied by the hand model chosen. Generally, the human hand is modeled with more than 20 DOFs. The second condition has to be evaluated for individual reduced marker set designs. In a model based approach, the geometry of the hand structure can be utilized to eliminate certain markers.

3.2 Instrumented Gloves

A second approach is to use non-vision based techniques to capture the motion of the hand. This can be done with the help of data gloves that utilize inertial, magnetic or resistive sensors to capture several kinds of measurements. Detailed information about specific hand movements like grip and pinch strength, sensitivity to temperature and vibrations and joint range of motion [12] can be used to augment traditional methods in assessing hand motion for designing robotic devices for grasping and manipulation. Instrumented gloves are very suitable for motion capture of the hands by using sensors as the sensors require to be placed on the hand stably, but unlike optical makers cannot be attached to hands directly due to their size and presence of cables. Furthermore, they are easy and comfortable to use, do not involve extensive preparation of the subject and have a pleasing outer appearance. Another option is to use physical frames made of metal, plastics etc., but they have the disadvantage of obstructing natural motion of hands in addition to preventing contact with the environment, and thereby loss of tactile feedback.

In order to capture the hand motion glove-based devices are usually developed to directly measure the joint angles and spatial positions by attaching a number of sensors to finger joints. Some commercially available products that are used to study the motion of fingers include the DataGlove family (Fifth Dimension Technologies (5DT), Irvine, CA), Cyberglove (Immersion Corporation, San Jose, CA), and the Humanglove^{TM} (Humanware S.R.L., Pisa, Italy) [17] (shown in Fig.3).

Figure 3. Commercially Available Glove-Based Devices: (a) Cyberglove (b) DataGlove (c) Humanglove

The Data glove measures finger flexures by means of flex sensors attached to the fingers. Quam et al. [18, 19] evaluated the glove by placing the hand in known positions and measuring the response of the glove sensors. They found that the mean error for the thumb sensors was 11 degrees with a standard deviation of 9 degrees, and the mean error of the finger sensors was 6 degrees with a standard deviation of 3 degrees.

Cyberglove II has eighteen sensors: two bend sensors on each finger, four abduction sensors, plus sensors measuring thumb crossover, palm arch, wrist flexion, and wrist abduction as long, thin strips sewn into the glove fabric that measure the change in resistance to an electric current as the sensor is bent. Kessler et al. discuss the Cyberglove as a whole hand input device [20]. They find that the repeatability of measurements from the device is dependent on both the joint being measured and the angle being measured.

The commercial Human Glove is equipped with 20 Hall-effect sensors to record flexion/extension and adduction/abduction of hand finger joints. Vecchi et al. [21] find

that the glove is able to furnish information about the trajectories of the fingers during the different performance of various grasping tasks by the subjects.

These gloved devices are typically equipped with a large number of sensors in order to capture much general information about the hands, and hence usually require interface units that translate the outputs of the sensors to recognizable form of information. The gloves retail at several thousand dollars each and are quite cost prohibitive. Traditionally, these gloves have been tethered to a data collection computer and have restricted the wearer's movements. However, some companies now offer a wireless connection between the glove and a nearby data collection computer, allowing the wearer to move freely within the room. Both 5DT and Immersion have released wireless versions of their gloves, which use Bluetooth® technology to transmit data to nearby computers. These wireless options can be expensive but give the wearer freedom to move about the home and community settings while data is being collected [17].

While the commercially available gloves are quite sophisticated and can provide a wide variety of information, these are not the optimal solution when only certain types and amounts of information are required to perform a task . Due to the wide-spread availability of small sized and low-cost microelectromechanical systems (MEMS) devices building dedicated systems to fulfill directed needs is a very attractive alternative. Thus, in addition to the many commercially available gloved devices, many non-commercial devices have been reported in literature. Some notable examples are: The Acceleration Sensing Glove (ASG) developed by Seth Hollar (Berkeley Sensor &

Actuator Center, University of California, Berkeley) [22], the Technische Universität

Berlin (TUB) sensor glove [23] and the Shadow Monitor [17] (shown in Fig. 4).
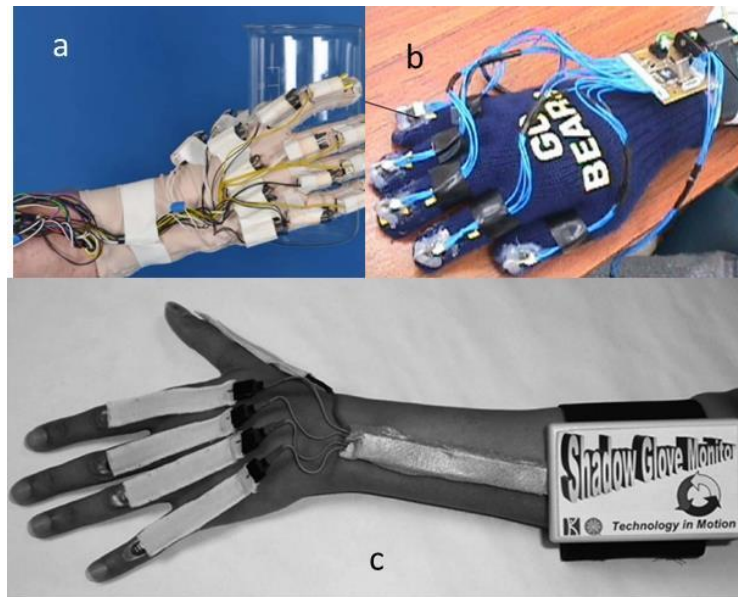
Figure 4. Noncommercial Instrumented Gloves: (a) TUB Glove, (b) ASG Glove, (c) Shadow Glove

The Acceleration Sensing Glove consists of six two-axis accelerometers placed

on the fingertips and back of the hand, and is used to detect and translate finger and hand

motion to interpretable signals. The sensors are connected to a controller boards

mounted on the wrist. The controller can then transmit the output of the sensors to the

data collection computer either through a cabled or wireless connection.

The Technische Universität Berlin (TUB) sensor glove is a flexible right-handed

device equipped with fourteen joint angle sensors. Gulke et. al [23] report a study with

forty-eight participants to assess whether there is a universal pattern of movement of the

finger joints while performing a certain gripping motion. They find that a flexion motion began either at the MIP or PIP joints, with the DIP joint always the last to move. Also, the sequence of the joints at the end of the gripping motion was different than the one at the beginning.

Simone et.al [17] developed the Shadow Monitor to allow unobtrusive measurements of finger joint flexion by using bend sensors. The glove is composed of sleeves attached to the back of the finger by double sided medical tape for each joint to be monitored, which contain the bend sensors. It also has the capability to store data locally on the device if transmission to a computer is not possible.

3.3 Discussion

As noted, a variety of sensors have been employed to measure joint angle, including accelerometers, bend sensors, flex sensors and Hall-effect sensors. For our purpose of synthesizing kinematic chains, as reported by Robson et al. [8-11], velocity and acceleration of the fingertips is required in addition to position data. While this information can be approximated by discrete time differentiations of position data obtained from the motion capture, inertial sensors like accelerometers can give direct measurement of the same. While an Inertial Measurement Unit (IMU) provides greater functionality, their sizes are two orders of magnitude larger than the commercially available accelerometer breakout boards. The size of the sensor is an important consideration for us as large sensors placed on the fingers impede their natural motion. Based on this consideration we choose to place accelerometer breakout boards on the

fingertips. Thus, we develop a sensor glove that consists of accelerometers attached to

the fingertips in addition to infrared markers to track the motion of the fingers.

4. PILOT DATA FROM AN EXISTING PRELIMINARY PROTOTYPE DEVICE

4.1 Device Description

Our aim is develop a device that helps us to obtain linear and angular positions, velocities and acceleration specifications of the fingertips. As mentioned earlier, the optical motion capture system can track the position of each marker in numeric coordinate values accurately in three dimensions. However, the derivatives (i.e. velocity and acceleration) can only be approximated from the discrete time differentiations, which induce quantization error. The noisy effect due to this error gets higher, especially when the captured movement is slow. In order to resolve this issue, inertial sensors can be applied for more accurate measurements of the higher order derivatives.

An inertial sensor or an accelerometer is self-contained device that does not require any external aids for its implementation. However, due to the lack of an external reference, accelerometer outputs tend to drift over time. Acceleration outputs have to be double integrated to obtain information about displacement, and measurement errors quickly build up to a significant misalignment between the calculated and the actual position. This difficulty of maintaining long-term stability still limits the field of application of inertial sensing as it usually requires additional information to produce meaningful data in the long term [24].

For our purpose, we use the accelerometers within an optical motion capture environment. In what follows, a preliminary prototype of metallic frame supporting multiple accelerometers is used to compare acceleration, velocity and position data obtained from the prototype device and Vicon (see Fig. 5). The prototype was developed

16

in the Human Interactive Robotics Lab at Texas A&M University by Hyosang Moon and Wyatt Smitherman and is equipped with an accelerometer breakout board on each fingertip and back of the hand to verify if the direct measurement on the acceleration can be used to enhance the accuracy in derivative data (i.e. velocity estimation and acceleration measurement) compared to the discrete time differentiations of the motion capture data (i.e. position measurement).

The ADXL335 tri-axis accelerometers, used in the device reported provide output voltage proportional to the linear acceleration in each axis. All output data from the accelerometer is given in terms of analog voltage, which varies from 0 V to 3.3 V as the acceleration varies from -3 g's to 3 g's. A Zero acceleration or zero-g offset present in this output is usually defined as the output voltage equal to half the supply voltage (3.3V/2 = 1.65 V). Voltages above 1.65 V signify acceleration and those below it signify deceleration. The output acceleration is calculated from the output voltage as:

$$Acceleration = (Output\ Voltage - Bias) * Sensitivity \qquad (1)$$

Sensitivity is found from the accompanying datasheet for the specific sensor used. Additionally, we know that acceleration data obtained from accelerometers is in the device local frame. In order to utilize the data obtained from the accelerometer in the base frame, located above the wrist, a transformation matrix between the accelerometer local frame and the desired fixed frame needs to be defined. When combining an accelerometer with optical motion capture, usually the accelerometer is placed in such a manner with optical markers such that the accelerometer local frame can be defined using these markers.

In the preliminary prototype, a metal bracket is placed on the top of each accelerometer board to attach three reflective markers to formulate a local frame aligned to the internal coordinate frame of the accelerometer.
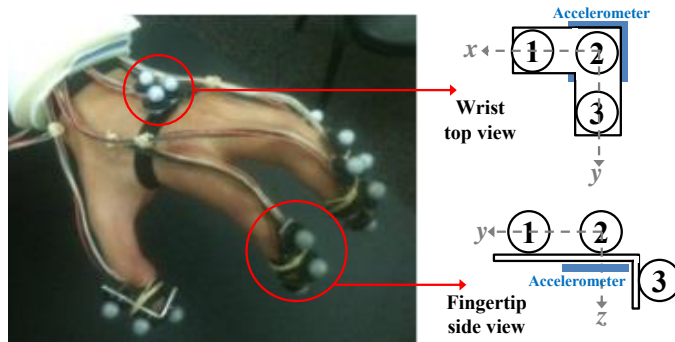
Figure 5. Preliminary Prototype Frame With Accelerometers, Attached Above the Wrist and Fingertips

4.2 Experimental Setup

The experimental setup consists of an optical motion capture system consisting of infrared emitter implemented cameras with reflective markers (Vicon, OMG Plc., UK). The software of this system captures the distance to each marker from multiple cameras and computes the 3D position with respect to the fixed coordinate system defined in the workspace volume by applying a triangulation method [25]. Accelerometer breakout boards (ADXL335, Adafruit Industries, USA) were used to measure acceleration of the fingertips. The Vicon analog channels are used to record the

raw acceleration values. All data was sampled at 100 Hz and all data processing is done in MATLAB (Math Works Inc., Natick, MA, USA).

To test the existing prototype device, preliminary experiments are carried out with a healthy young adult. The subject was seated at a table with the right hand, encased in the prototype being tested, placed on top of the table (Fig. 6). During the experiment, the subject performed a light grasping task repeated for several times.
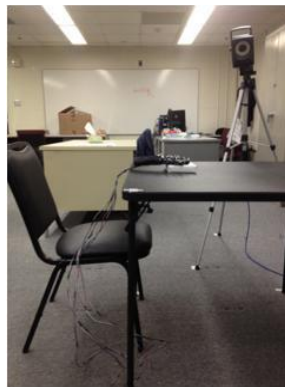
Figure 6. Experimental Setup

4.3 Comparison of Linear Acceleration Data Obtained from Accelerometers versus from Vicon Motion Capture System

For each location, the prototype can directly measure the position from the marker and acceleration from the accelerometer. In order to approximate the optimal velocity value, Kinematic Kalman Filter (KKF) is applied. Since the KKF derives the optimal state estimation based on the kinematic model instead of uncertain physical model, the velocity can be estimated under an ideal condition [26]. The kinematic model

of data glove prototype (see Fig. 7) in a state space representation can be obtained as [26]:

$$x_{k+1} = Ax_k + B(a_k + n_k)$$
$$y_{k+1} = Cx_k + m_k \qquad (2)$$
$$A = \begin{bmatrix} 1 & T_s \\ 0 & 1 \end{bmatrix}, B = \begin{bmatrix} \dfrac{T_s^2}{2} \\ T_s \end{bmatrix}, C = \begin{bmatrix} 1 & 0 \end{bmatrix}$$

Where, a_k and n_k are the measurement and the noise of the accelerometer output, respectively and m_k refers the quantization noise of the optical motion capture system. The steady state Kalman filter is designed by the discrete time algebraic Riccati equation (see [26] for more detailed explanations).

Figure 7 compares the KKF estimation with the motion capture system measurement and its numerical differentiations for a selected experimental trial. During the experiment, a subject performed a light grasping task repeated for several times. As shown in Fig. 7(c), the accelerometer measurement and the second order discrete time differentiation of the motion capture system have deviations. The velocity estimations from the motion capture system and the KKF show a little difference (see Fig. 7(b)).
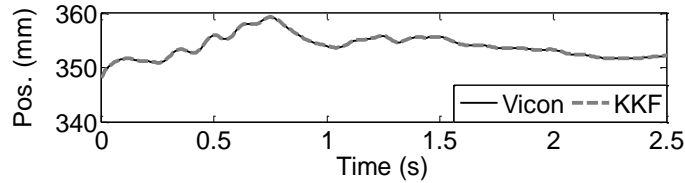
(a) Position comparison
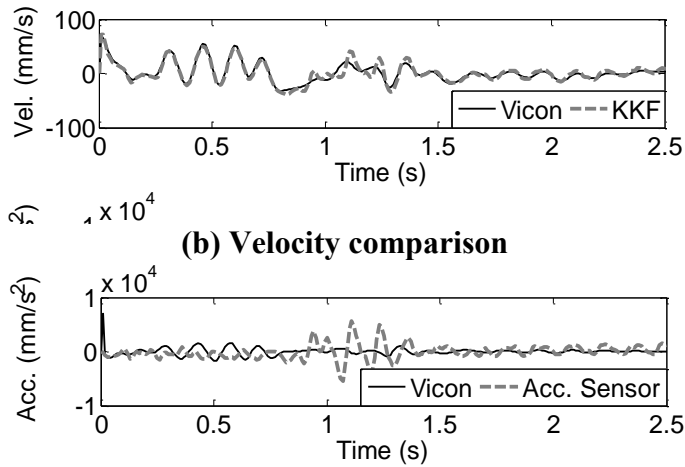
(b) Velocity comparison

(c) Acceleration comparison
Figure 7. Comparison between KKF state estimation and the Vicon Motion Capture System Measurement from a repeated light hand grasping task. Dataset of Vertical direction (z-axis) on the ring finger is used.

4.4 Discussion

The preliminary prototype device verifies the usefulness of accelerometers in a motion-capture system for fine movements. The implementation of accelerometers results in improvements in capture of acceleration and velocity information by eliminating time-lags that occur through ordinary differentiation methods, and indirect filtering. The effect of low-pass filtering employed in Vicon systems on accelerations obtained by differentiating position data is briefly discussed by Thies et al. [27]. The authors compare linear accelerations obtained from inertial accelerometer sensors and by double differentiation of position data from the Vicon system for gross movements of the arms. They found good correspondence between the two methods for 'reach and grasp' tasks. They propose that the low-pass filtering of marker data in the Vicon system results in lower noise in the acceleration obtained by differentiating Vicon data than in

21

the data from the accelerometers. Based on this they suggest adding a representative measure of noise to Vicon data to obtain simulation of accelerometer by the Vicon.

We find that the use of accelerometers provides us with acceleration data that is free from problems attendant with capturing motion with a large number of markers such as missing marker data or temporary misidentification etc.

Additionally the position sensing resolution of the Vicon motion capture system setup was computed as 0.8 mm according to the specifications shown in the system reference (Vicon MX Hardware) and the equation to derive the geometric spread of a point on the projected image on the sensor [28]:

$$\sigma = r\left(1 + \frac{f}{d}\right) \tag{3}$$

Where, σ is the resolution of the motion capture system, r (=0.8 mm) represents the diameter of the camera sensor aperture, f (=16 mm) indicates the focal length of the camera lens, and d (=4,000 mm) is the distance from the camera to the object of interest. Initially, we expected noisy signals for the velocity and acceleration calculations of the motion capture system due to magnified quantization errors. The reason for such small deviations may be due to 10^{-6} mm digits output representation of the Vicon motion capture system.

However, we find a significant mismatch between the accelerations obtained from the accelerometers with those calculated in the Vicon system. We hypothesize that this arises from imperfect transformation of accelerometer data from the moving frames to the base frame. This issue is addressed in detail in the following section.

While the prototype device is able to obtain position, velocity and accelerations of the fingertips, no information is available regarding joint angles. While calculation of joint angles can be accomplished by attaching additional markers on the hand in addition to the device, it will create many practical problems due to occlusion (due to presence of frame, wires and a large number of markers) and restriction in natural motion. The preliminary prototype design, which attaches a frame on the fingertips, restricts natural motion by degrading the quality of tactile feedback to the fingertips when in contact with an object.

From the above discussion it is clear that any device used to collect information regarding the position, velocity, acceleration of the hand the device should not affect the hand's ability to interact with objects in the environment. In the next section, a new experimental prototype of a sensor-based glove is proposed and developed and discussed, addressing the outlined shortcomings.

5. DEVELOPMENT OF A SENSOR-BASED GLOVE FOR CAPTURING HUMAN HAND KINEMATICS DATA

5.1 Device Description

In this section we discuss the development of a sensor glove for capturing the motion of the fingers. The creation of effective custom measurement systems requires initial detailing of requirements. While it may be tempting to solve multiple problems with one system, this often leads to overly complicated devices that take too long to complete, and may not actually meet the core requirements [29]. For the sensor glove, we require that the device must be able to provide information about the position, velocity and acceleration of the fingertips. However, to avoid problems with motion capture, it should not have more than the minimum required number of infrared markers to allow reconstruction of hand poses with sufficient accuracy. Also, while the glove should provide a snug fit so that the sensors capture the motion of the hand accurately, it should not impede the natural motion of the hands. Finally, the glove must be easy to don and remove, and sensors and their wirings should not cause any physical discomfort for the user.

5.2 Reduced Marker Protocol

To address the issue of using the minimum number of infrared markers, we begin by formulating a reduced marker protocol. The challenge of tracking the motion of human hand arises from the difficulty of tracking the large number of DOFs of hand and finger motions without any hindrances in the optical motion capture system. Usually

markers are attached on every finger and hand joint and this makes motion capture troublesome due to problems like occlusion. The formulation of a marker set to capture the kinematics of the hand is highly dependent on the hand model selected. As has been discussed previously, the human hand is a highly complex structure and many models have been formulated to represent it. In this section we present an abbreviated form of the most commonly used 27 DOF kinematic model of human hand. In this model, each finger has 4 DOFs except for the thumb, which possesses 5 DOFs. As a preliminary work, we only consider four fingers connected at the wrist except the thumb, which has different kinematic structure from the other fingers (see Fig. 8).
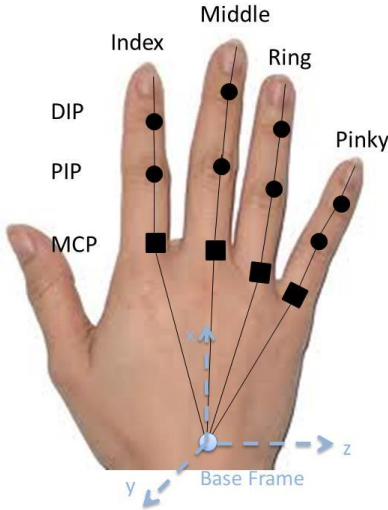

Figure 8. Kinematic Structure of Human Hand. ■ and ● Represent a Universal (T) and a Revolute Joint (R), Respectively.

In order to represent the motion kinematics, a base or fixed frame (frame F) is defined on the back of the hand and each finger is modeled as a 4 DOFs serial kinematic chain. The metacarpophalngeal (MCP) joints, which connect the fingers to the palm, are represented as universal joints (i.e. 2 DOFs: flexion-extension and abduction-adduction). The proximal interphlangeal (PIP) and distal interphalngeal (DIP) joints are modeled as revolute joints (i.e. 1 DOF: flexion-extension). At the distal end of the finger, fingertip location is defined to represent the motion of end link of each finger.

For the protocol, we identify the markers that are indispensable for reconstruction of the hand pose. In order to define a local frame on the back of the hand, at least three markers are required. Additionally, the definition of the plane of motion of the finger requires the placement of a minimum of three markers on each finger. Of these, a marker has to be necessarily placed on the fingertip to describe the position of the sensors. Based on this, as an initial idea, we simplify the problem by not attaching a marker on DIP joint location as shown in Fig. 9. In order to fully describe the kinematics of the finger, the missing DIP joint position has to be derived from the geometry of the finger linkage. Prior to the inverse kinematics implementation, it is assumed that 1) the motion of each serial chain is constrained on a 2D plane defined by TIP, PIP and MCP marker positions (i.e. axes for all revolute joints are aligned parallel) and 2) no three markers on a finger are collinear, which appears to be true for natural postures. In this sense, the lateral movements of the finger linkage is solely generated by the adduction-abduction angles at the MCP joint with respect to the local coordinate frame.
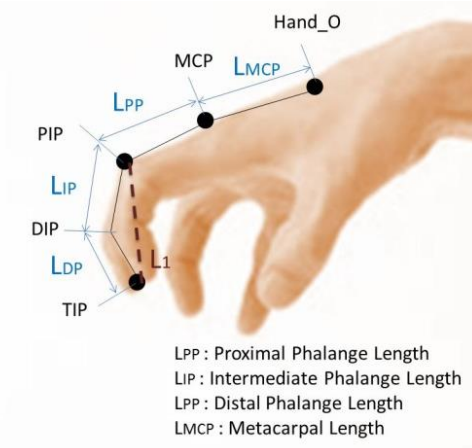
Figure 9. Configuration of the Proposed Initial Idea of the Reduced Marker Protocol on the Index Finger

For the inverse kinematics, we first form a triangle with TIP, DIP and PIP locations (see Fig. 9). From the geometry of the linkage, the angle of DIP can be obtained by the law of cosine as:

$$\theta_{DIP} = \cos^{-1}\left(\frac{L_{IP}^2 + L_{DP}^2 - L_1^2}{2L_{IP}L_{DP}}\right)$$

(4)

Where, L_{IP}, L_{DP} and L_1 represent the length of each side in the triangle (see Fig. 9 for clarification). The anatomical lengths, L_{IP} and L_{DP} can be physically measured, while the varying distance L_1 can be computed from the positions of the markers at TIP and PIP. Additionally, the function arccosine function has two solutions, of which one is rejected on the basis of the natural constraints of the human hand described by Lin et al. [3] as:

$$0^o \leq \theta_{DIP} \leq 90^o$$

(5)

From the known values, the hypothetical DIP marker position is estimated by solving a system of constraint equations below:

27

$$L_{DP} = \left\| \mathbf{x_{TIP}} - \mathbf{x_{DIP}} \right\|$$
$$L_{IP} = \left\| \mathbf{x_{MCP}} - \mathbf{x_{DIP}} \right\| \tag{6}$$

Where, $\mathbf{x_{TIP}}$, $\mathbf{x_{DIP}}$ and $\mathbf{x_{MCP}}$ indicate the position vector for each TIP, DIP and MCP marker. Here, $\|\cdot\|$ refers the norm of the vector inside it. By solving Eq. 6 for $\mathbf{x_{DIP}}$, the position of hypothetical DIP marker can be obtained. Once the position of the missing DIP marker is known, the full kinematics and the pose of finger can be derived.

5.3 Extraction of Acceleration Data

In this sub-section we address the question of transforming the accelerometer data from the local device frame to a fixed base frame. To do this, we first briefly describe some concepts of spatial geometries. A frame is defined as a set of four vectors giving position and orientation information of a point in three dimensions. To define an orthogonal coordinate frame, three non-collinear points (A, B, C) are required. A system of three unit, mutually orthogonal vectors centered at point A is obtained by:

$$v1 = B - A;$$

$$v1 = v1/norm(v1);$$

$$v3 = cross(v1, C - A); \tag{7}$$

$$v3 = v3/norm(v3);$$

$$v2 = cross(v3, v1);$$

The new coordinates of a point P (originally in the world frame) in the newly defined frame F can be obtained as:

$$^{F}P = [dot(P - A, v1), dot(P - A, v2), dot(P - A, v3)] \tag{8}$$

Where, dot(A,B) denotes the vector dot product operation.

In the preliminary device described in the previous section, the accelerometer is placed on a metal bracket with three infrared markers that help to define the accelerometer local axes. In the design of the glove, we chose to forego the use of frames in order to obtain more natural motion of the hands. The glove utilizes the three markers placed on each finger to locate a local coordinate system centered on the fingertip markers (Frame L2). An additional frame (Frame L1) centered at the MCP joint is also defined. The axes of frame L2 are carefully defined such that they are aligned as closely as possible with the accelerometer local axes as shown in Fig. 10.
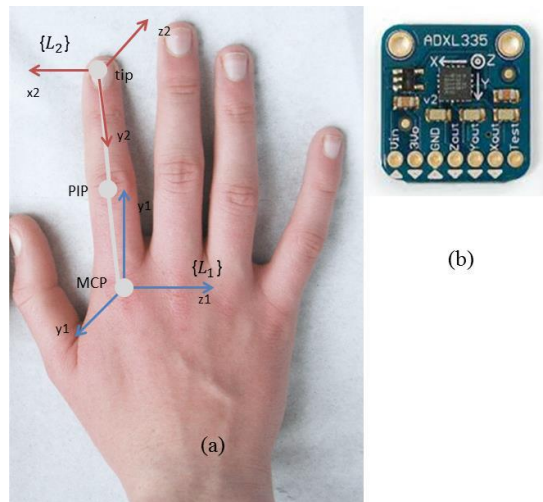

Figure 10. (a) Pictorial Depiction of Frames L1 and L2 Along (b) The local Axes of the ADXL 335 Device

As accelerometer outputs are given in their own local frame, the accelerometer data obtained is the local acceleration, i.e. acceleration taken in the coordination frame of the fingertip which moves with the fingertip. In order to determine accelerations in the fixed frame L1, a transformation matrix must be obtained to transform the data from the moving frame L2 to the fixed frame L1. In the moving frame, acceleration data is obtained from the sensor and velocity and position information is obtained by integrating the accelerometer outputs in MATLAB. In the fixed frame, the position data is obtained from the markers and time differentiation yields velocity and acceleration information. Once all the required information is defined on a common frame of reference, we proceed to the next stage of calculations.

5.4 Coordinate Planar Displacements

In this section we describe the derivation of a relative position homogeneous transformation matrix as presented by McCarthy and Soh [31]. Any point **p** in a moving frame L2 can also be written as **P** in a fixed coordinate frame L1. If the origin of the frame L2 coincides with the origin of frame L1, and the angle between the x-axes of these two frames is ϕ as shown in Fig. 11, then the coordinates of **P** are given by:
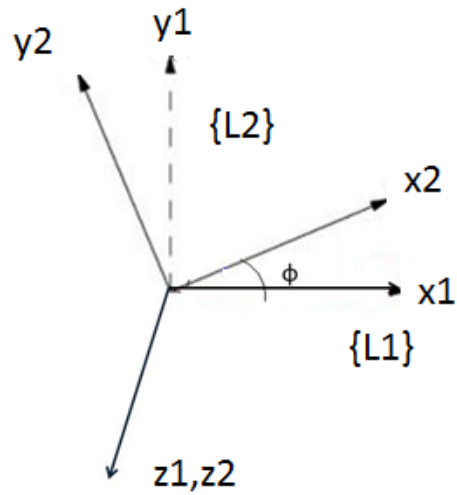
Figure 11. Rotation operator

$$\begin{bmatrix} P \\ 1 \end{bmatrix} = \begin{bmatrix} c\phi & -s\phi & 0 \\ s\phi & c\phi & 0 \\ 0 & 0 & 1 \end{bmatrix} \begin{bmatrix} P \\ 1 \end{bmatrix} \tag{9(a)}$$

$$[Z(\phi)] = \begin{bmatrix} c\phi & -s\phi & 0 \\ s\phi & c\phi & 0 \\ 0 & 0 & 1 \end{bmatrix} \tag{9(b)}$$

Where,

$c\phi = cos\phi,$

$s\phi = sin\phi$

$[Z(\phi)]$ = Rotation Matrix

On the other hand, if the origin of the moving frame L2 is displaced by **d** from the origin of the fixed frame L1, but $\phi = 0$ as shown in Fig. 12, then
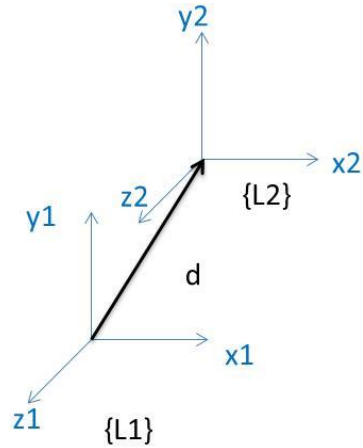
Figure 12. Translation Operator

$$\begin{bmatrix} P \\ 1 \end{bmatrix} = \begin{bmatrix} 1 & 0 & dx \\ 0 & 1 & dy \\ 0 & 0 & 1 \end{bmatrix} \begin{bmatrix} p \\ 1 \end{bmatrix} \tag{10(a)}$$

$$[X(d)] = \begin{bmatrix} 1 & 0 & dx \\ 0 & 1 & dy \\ 0 & 0 & 1 \end{bmatrix} \tag{10(b)}$$

Where,

dx = x-component of vector **d** from origin of frame L1 to origin of frame L2

dy = y-component of vector **d** from origin of frame L1 to origin of frame L2

[X(d)] = Translation Matrix

Combining the above two results, it is known that for a given point **p** in a moving frame L2, the coordinates of the corresponding point **P** in the fixed frame (as shown in Fig. 13) can be found by using a relative position homogeneous transformation matrix, T.
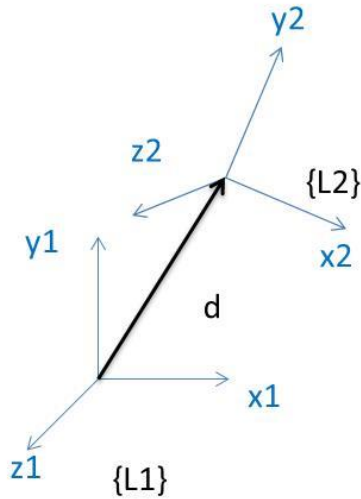
Figure 13. Homogeneous Transformation Operator

$$T = [Z(\phi)] \times [X(d)] \tag{11(a)}$$

$$T = \begin{bmatrix} c\phi & -s\phi & dx \\ s\phi & c\phi & dy \\ 0 & 0 & 1 \end{bmatrix} \tag{11(b)}$$

In addition to a relative position homogeneous transformation matrix, Robson & McCarthy [9] explain the derivation of a relative velocity homogeneous transformation matrix Ω and a relative acceleration homogeneous transformation matrix Λ.

The matrix Ω is used to obtain the velocity **V** of a point in a fixed frame L1, when the velocity of the point is given by **v** in the moving frame L2.

$$\boldsymbol{V} = \Omega \times \boldsymbol{v} \tag{12(a)}$$

Where,

$\boldsymbol{V}$ = velocity of fingertip in fixed frame L1

$\boldsymbol{v}$ = velocity of fingertip in moving frame L2

33

A relative velocity homogeneous transformation matrix Ω can be derived from the **T** matrix as:

$$\Omega = \dot{T} \times T^{-1} \qquad \text{(12(b))}$$

On differentiating T, we get:

$$\dot{T} = \begin{bmatrix} -\dot{\phi}.s\phi & -\dot{\phi}.c\phi & \dot{dx} \\ \dot{\phi}.c\phi & -\dot{\phi}.s\phi & \dot{dy} \\ 0 & 0 & 0 \end{bmatrix} \qquad \text{(12(c))}$$

We assume that $\dot{\phi} = 1$, i.e. constant angular velocity, then

$$\dot{T} = \begin{bmatrix} -s\phi & -c\phi & \dot{dx} \\ c\phi & -s\phi & \dot{dy} \\ 0 & 0 & 0 \end{bmatrix} \qquad \text{(12(d))}$$

And

$$\Omega = \begin{bmatrix} 0 & -1 & \dot{dx} + \dot{dy} \\ 1 & 0 & \dot{dy} - \dot{dx} \\ 0 & 0 & 0 \end{bmatrix} \qquad \text{(12(e))}$$

Finally, the relative acceleration homogeneous transformation matrix Λ can give the acceleration of a point in the fixed frame (**A**) given the acceleration of the corresponding point (**a**) in a moving frame. The matrix Λ can be used as:

$$\boldsymbol{A} = \Lambda \times \boldsymbol{a} \qquad \text{(13(a))}$$

Where,

$\boldsymbol{A}$ = acceleration of fingertip in fixed frame L1

$\boldsymbol{a}$ = acceleration of fingertip in moving frame L2

The matrix Λ is given by:

$$\Lambda = \dot{\Omega} + \Omega^2 \tag{13(b)}$$

To derive the matrix Λ, we first differentiate Ω to get

$$\dot{\Omega} = \begin{bmatrix} 0 & 0 & \dot{dy} + \ddot{x} \\ 0 & 0 & -\ddot{x} + \dot{dy} \\ 0 & 0 & 0 \end{bmatrix} \tag{13(c)}$$

And

$$\Omega^2 = \begin{bmatrix} -1 & 0 & dx - \dot{dy} \\ 0 & -1 & dy + \dot{dx} \\ 0 & 0 & 0 \end{bmatrix} \tag{13(d)}$$

Combining the two, we get

$$\Lambda = \begin{bmatrix} -1 & 0 & dx + \ddot{x} \\ 0 & -1 & dy + \ddot{y} \\ 0 & 0 & 0 \end{bmatrix} \tag{13(e)}$$

5.5 Position, Velocity and Acceleration Homogeneous Transformations for a Planar Two Degrees-of-freedom RR Kinematic Chain

Knowing the structure of the relative position, velocity and acceleration homogeneous transformation matrices between a fixed and a moving frame, we now extend the idea to a planar RR open chain. A planar RR open chain is defined by McCarthy and Soh [31] as having a fixed revolute joint O (see Fig. 14) that connects a rotating link to the ground link. A second revolute joint A connects the rotating link to the end-link, or floating link.

Let $\theta 1$ be the angle measured from x-axis of the fixed frame L1 to OA as the linkage moves, and let $\theta 2$ be the angle measured from OA to x-axis of moving frame L2. Then a point **p** in L2 is defined in L1 as:
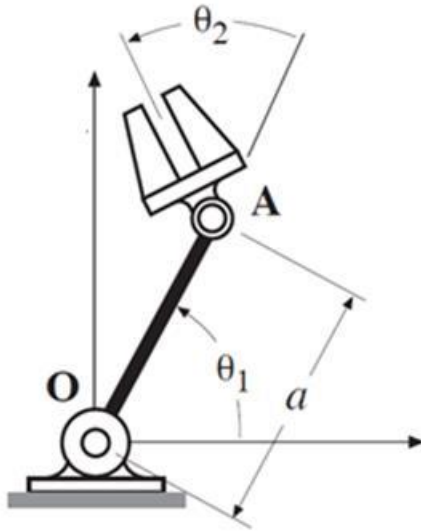
Figure 14. RR Open Chain

$$\boldsymbol{P} = [Z(\theta_1)] \times [X(d)] \times [Z(\theta_2)]\mathbf{p} \tag{14(a)}$$

$$T = \begin{bmatrix} c\phi & -s\phi & a.s1 \\ s\phi & c\phi & a.c1 \\ 0 & 0 & 1 \end{bmatrix} \tag{14(b)}$$

Where,

$\phi = \theta_1 + \theta_2$

$s1 = sin\theta_1$

$c1 = cos\theta_1$

The matrix Ω is given by:

$$\Omega = \begin{bmatrix} 0 & -1 & \dot{a}.s1 + a.c1 - a.c1.\dot{\theta}_1 \\ 1 & 0 & \dot{a}.c1 - a.s1 - a.s1.\dot{\theta}_1 \\ 0 & 0 & 0 \end{bmatrix} \tag{15(a)}$$

Now, a = constant, so $\dot{a} = 0$;

$$\Omega = \begin{bmatrix} 0 & -1 & a.c1 - a.c1.\dot{\theta}_1 \\ 1 & 0 & -a.s1 - a.s1.\dot{\theta}_1 \\ 0 & 0 & 0 \end{bmatrix} \tag{15(b)}$$

And the matrix Λ is given by

$$\Lambda = \begin{bmatrix} -1 & 0 & a.s1 - a.s1.\dot{\theta}_1^2 + a.c1.\ddot{\theta}_1 \\ 0 & -1 & a.c1 - a.c1.\dot{\theta}_1^2 - a.s1.\ddot{\theta}_1 \\ 0 & 0 & 0 \end{bmatrix} \tag{16}$$

5.6 Position, Velocity and Acceleration Homogeneous Transformations for a Planar Three Degrees-of-freedom RRR Kinematic Chain

Similarly the matrices T, Ω and Λ can be derived for a RRR open chain. If the distance a between the joints of an RR chain is allowed to vary, it gives rise to a 3 DOF planar manipulator. If this variation in length is modeled by a revolute joint, it forms a RRR open chain as shown in Fig. 15 [31].

Figure 15. RRR Open Chain

Let θ1 be the angle measured from x-axis of the fixed frame L1 to OE as the linkage moves, and let θ2 be the angle measured from OE to x-axis of an intermediate frame, and θ3 is the angle measured from OA to x-axis of moving frame L2. Then a point **p** in L2 is defined in L1 as:

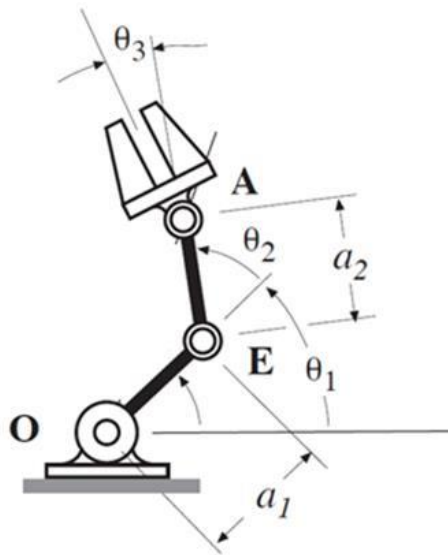$$\boldsymbol{P} = [Z(\theta_1)] \times [X(a1)] \times [Z(\theta_2)] \times [X(a2)] \times [Z(\theta_3)]\mathbf{p} \qquad (17(\text{a}))$$

$$T = \begin{bmatrix} c\phi & -s\phi & a1c1 + a2c12 \\ s\phi & c\phi & a1s2 + a2s12 \\ 0 & 0 & 1 \end{bmatrix} \qquad (17(\text{b}))$$

Where,

$\phi = \theta1 + \theta2 + \theta3$

$c12 = \cos(\theta1 + \theta2)$

$s12 = \sin(\theta1 + \theta2)$

As a1, a2 = constant; $\dot{a1} = 0$; $\dot{a2} = 0$

The matrix Ω is given by:

$$\Omega = \begin{bmatrix} 0 & -1 & -a1.s1.\dot{\theta}_1 - a2.s12.\dot{\theta}_{12} + a1.s2 + a2.s12 \\ 1 & 0 & a1.c2\dot{\theta}_2. +a2.c12.\dot{\theta}_{12} - a1.c1 - a2.c12 \\ 0 & 0 & 0 \end{bmatrix} \qquad (18)$$

Where, $\theta12 = \theta1 + \theta2$

$\dot{\theta}1$ and $\dot{\theta}2$ are obtained by time differentiation of $\theta1$ and $\theta2$.

Then, Λ becomes

$$\Lambda = \begin{bmatrix} -1 & 0 & a1.c1 + a2.c12 - a1.c1.\dot{\theta}_1^2 - a1.s1.\ddot{\theta}_1 - a2.c12.\dot{\theta}_{12}^2 - a2.c12.\ddot{\theta}_{12} \\ 0 & -1 & a1.s2 + a2.s12 - a1.s2.\dot{\theta}_2^2 - a2.s12.\dot{\theta}_{12}^2 + a1.c2\ddot{\theta}_2 + a2.c12.\ddot{\theta}_{12} \\ 0 & 0 & 0 \end{bmatrix} \qquad (19)$$

5.7 Application of the Position, Velocity and Acceleration Homogeneous Transformations to a Planar Three Degrees-of-freedom Finger

In this sub-section, we will show how the information collected from the glove allows us to define the position, velocity and acceleration transformation matrices, when the finger is approximated to three degrees of freedom RRR chain as shown in Fig 16 (b). The motion of the DIP joint is constrained and the DIP angle is assumed to be a constant. Comparing part (a) and (b) of Fig. 16, we see that a1, a2 and s can be obtained from the markers placed on the hand as:

$$\boldsymbol{a1} = PIP_{marker} - MCP_{marker};$$

$$\boldsymbol{a2} = TIP_{marker} - PIP_{marker}; \qquad\qquad (20)$$
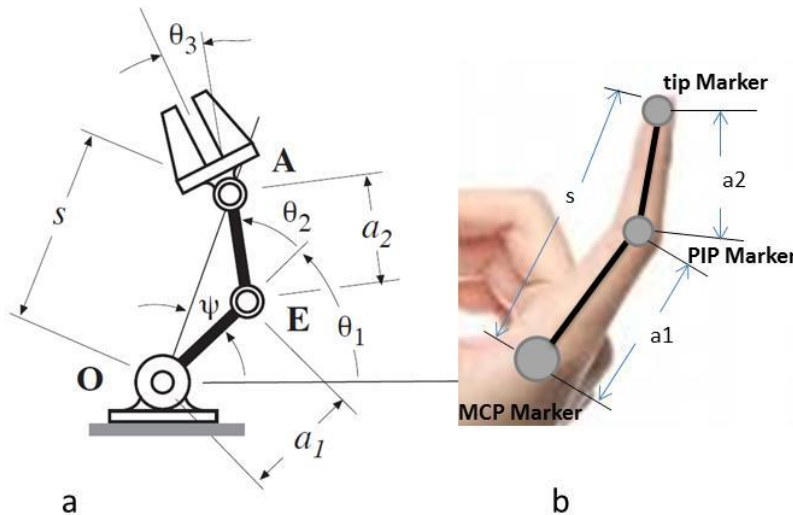
$$\boldsymbol{s} = TIP_{marker} - MCP_{marker};$$

Figure 16. Transformation Operators for a 3DOF Finger: (A) RRR Chain (B) Equivalent Link Parameters

Then angle θ2 can be obtained using the following equation.

$$\theta_2 = \cos^{-1}\left(\frac{s^2 - a1^2 - a2^2}{2.\,a1.\,a2}\right) \tag{21}$$

To select one of the two values suggested by the arccos function, we impose a further constraint:

$$0^o \leq \theta_2 \leq 90^o \tag{22}$$

Also,

$$\psi = \tan^{-1}\left(\frac{a2.\sin\theta2}{a1 + a2.\cos\theta2}\right) \tag{23}$$

And,

$$\theta1 = \tan^{-1}\left(\frac{s_x}{s_y}\right) - \psi \tag{24}$$

Assuming ϕ is known,

$$\theta3 = \phi - \theta1 - \theta2 \tag{25}$$

In the following subsection we describe some experiments that were carried out to observe the difference between the coordinates of the fingertip in the fixed frame calculated by using the transformations with those obtained from the Vicon.

5.8 Experimental Set Up and Testing

The same experimental setup as described in the previous section is used. The proposed initial idea of a reduced marker protocol is tested by an experiment carried out with a healthy young adult. The subject was seated at a table with the right hand, encased in the glove, placed on top of the table. The gloved device is shown in Fig. 17.

A cuboidal object is placed on the table directly in front of the subject. The motion of the subject trying to grasp the test piece is recorded.

Figure 17. Glove-Based Prototype Device (A) Glove Without Markers (B) Glove With Markers Attached

In a second set of experiments we compare the extracted acceleration data from the sensors with time double differentiation of position data. For this experiment, the subject is given the task of squeezing a stress ball placed on the table in front of them as shown in Fig 18.
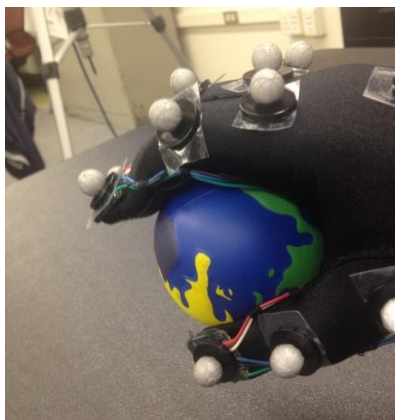
Figure 18. Subject Squeezing a Stress Ball

Experiment I: Full marker configuration is applied on a human subject's hand (i.e. TIP, DIP, PIP and MCP) and the angle of DIP joint is computed both from the measured and the estimated DIP joint positions. The data collected is processed in MATLAB and Fig. 19 shows the difference between the DIP angles that are obtained from the full marker set and the reduced marker set. The mean of RMSE (root mean square error) between two values was 2.1° with a standard deviation of 1.05° over five trials recorded.

Figure 19. Comparison Between Calculated DIP Angle of Index Finger Obtained From Proposed Reduced Marker Protocol and Full Marker Set.

The main source of error can be attributed to the inaccuracy in the measurements of the phalangeal link lengths (i.e. L_{DP} and L_{IP}). It is likely that the link lengths' estimation is sensitive to the TIP and PIP marker positions which contain the intrinsic

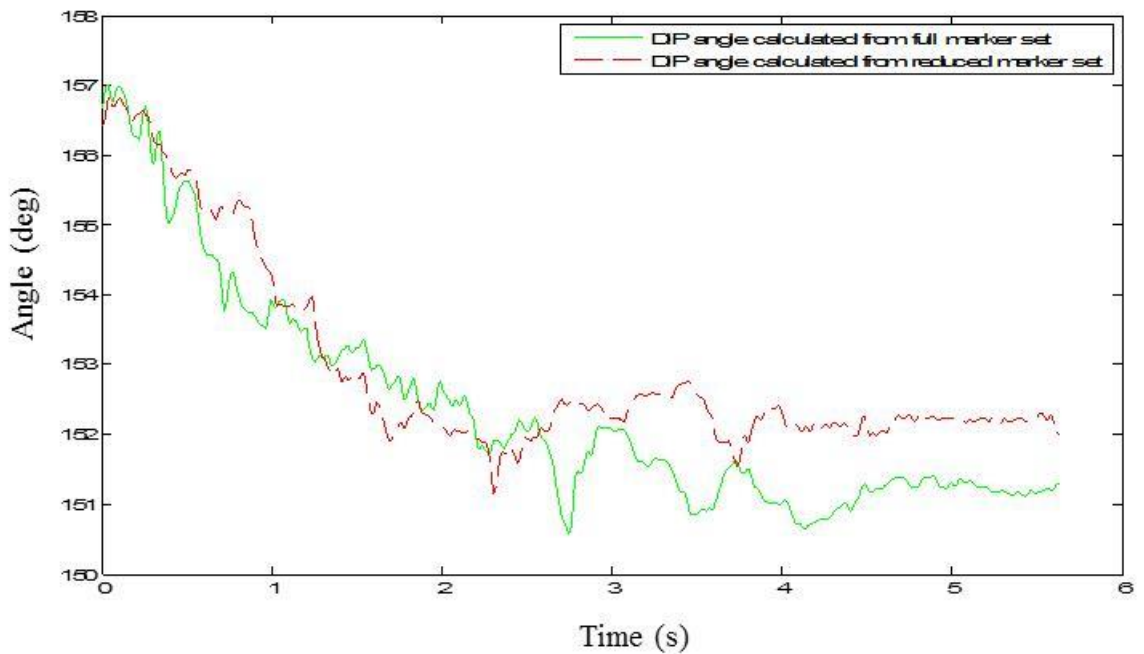measurement errors such as relative movement of the marker on the skin. Although the proposed method shows lower accuracy than the conventional full marker configuration method, it can reduce up to 4 markers in the full hand configuration shown in Fig. 9. In addition, by replacing some of the markers with inertial measurement systems, we can expect less obstructive experiments than the conventional optical motion capture method.

Experiment II: The sensor affixed on the fingertip gives provides acceleration information in the device local frame every 0.01s. This acceleration is integrated to obtain velocity, which in turn on integration provides the position information for the fingertip in the local frame. By using the relative homogeneous transformation matrices derived in Eq. 17, 18 and 19, we obtain corresponding acceleration, velocity and position of the fingertip in fixed frame L1. The optical motion capture data gives the position of the fingertip in the fixed frame, which on differentiation yields velocity and acceleration.
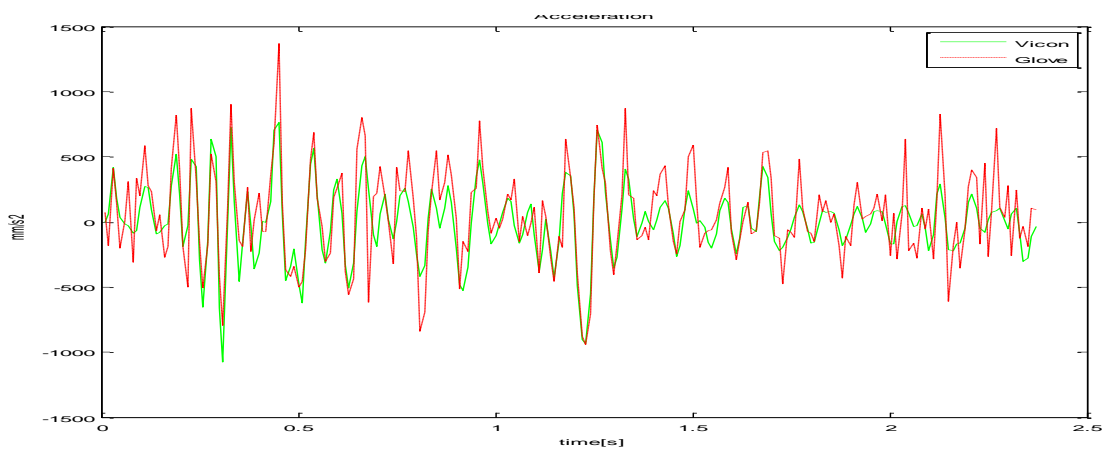
(a)

Figure 20. Comparison between estimated (a) acceleration, (b) velocity and (c) position of fingertip in a fixed frame and the Vicon Motion Capture System Measurement.
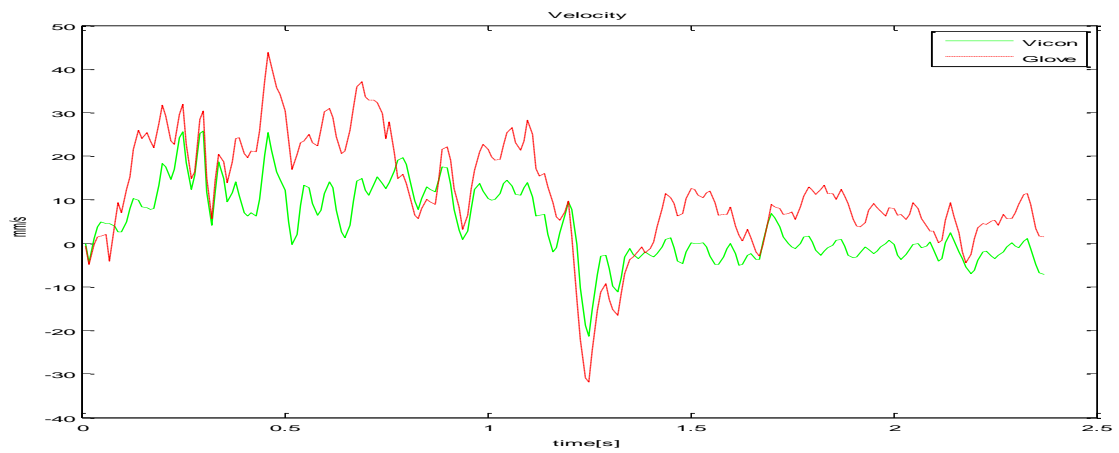
(b)
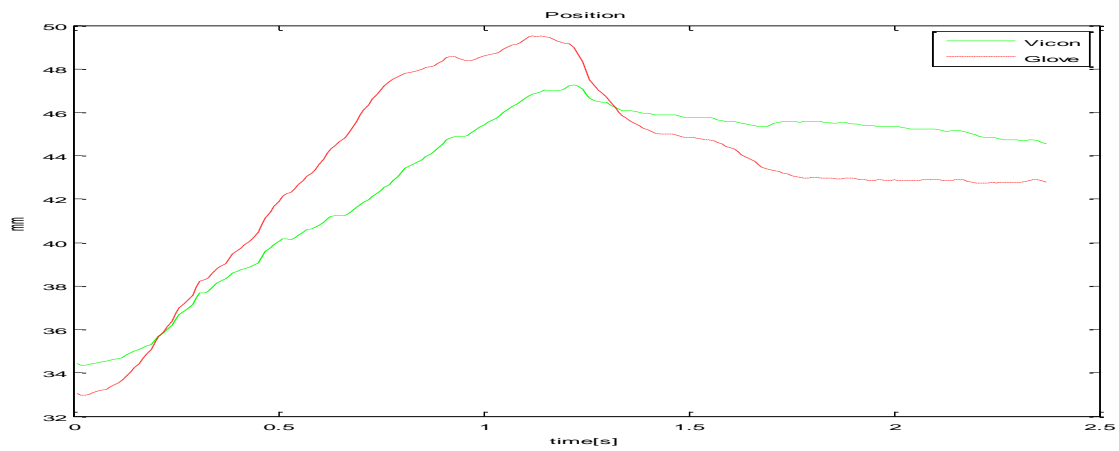
(c)

Figure 20. Continued.

We find that the linear acceleration trajectories obtained from the glove closely resembles that obtained from the Vicon system. We note that the use of relative acceleration homogeneous transformation matrix enables us to get acceleration values closer to those obtained from Vicon, as compared to the results reported in Section 4

44

using the preliminary device. The accelerations obtained from the glove show more noise than that obtained from the Vicon, and the Root Mean Squared (RMS) errors are 190 mm/s^2. The velocity and position obtained from the glove differs from that given by the Vicon system in the Frame L1 by 50 mm/s, 1.5 mm respectively. The data shown in Fig. 20 corresponds to the x-axis of fixed frame on the index finger. The difference in velocity and position estimation can be attributed to errors due to integration. In the future, we expect that these errors can be significantly reduced by additionally employing Kalman Filters for optimal velocity and position estimation. Thus, the fully developed glove is expected to provide accurate estimation of the movement of the hands, even in trials with missing or misidentified marker data.

6. APPLICATIONS

The current section presents recent efforts on using first and second order task constraints, compatible with contact and curvature specifications between the fingers and a grasped object, in the design of planar and spatial kinematic chains. These constraints are based on data obtained from the sensor-based glove reported in the thesis.

6.1 Planar Example: Design of a Human-like Finger for Anthropomorphic Task

Our first example discusses the design of a planar anthropomorphic RRR kinematic chain, for which link lengths have been defined directly from measurements of the index finger of a human subject. In order to test the performance, the manipulation of a stress ball task was performed, presented in detail in the previous chapter.

6.1.1. Task Specification

During the task, the subject emulates grasping and squeezing motion. The arm kinematics is captured by 3D Motion Capture System (Vicon, OMG Plc., UK). In the motion capture system, three infrared cameras track the position of each reflective marker attached on the subject's finger relative to the predefined global coordinate with 100Hz sampling rate. Four moving frames are defined each at each joint of the index finger and the tip of the index finger. Fig. 21 shows the marker attachment and its kinematic structure developed in the 3D Motion Capture System. In order to count only for the finger motion, the linear and angular kinematics (i.e. positions and velocities and accelerations) of each moving frame are computed with respect to the fixed frame, located at the back of the hand.
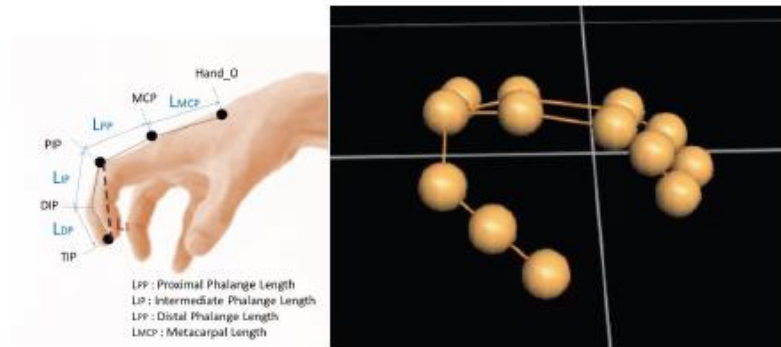
Figure 21. Human Hand Joint Marker Positions and Their View From the Vicon Motion Capture System

The task positions, contact direction and second order motion constraints, determined from the subject's motion, are listed in Table 1.

Table 1. The Two Task Positions, Two Velocities and One Acceleration for the Fingertip of the Planar RRR Kinematic Chain, Obtained From the Developed Data-Glove.

Task	1	2
Position $(\theta°, x, y)$	$(-117.38, -77.71, -43.91)$	$(-100.42, -70.50, -53.06)$
Velocity $(\omega°/s, v_x, v_y)$	$(24.06, 7.86, -22.74)$	$(0.02, -0.01, -0.01)$
Acceleration $(\alpha°/s^2, a_x, a_y)$	-	$(-109.91, -29.67, -12.35)$

The task consists of an initial position and velocity, which defined by the hand start position and hand start velocity, as well as a second position and velocity, defined as the contact position and contact velocity, respectively. The acceleration in the second

47

position is defined with the main goal of maintaining the contact between the fingertip and the ball in the vicinity of the grasped/second position.

6.1.2. Synthesis Results

Figure 22 presents the results from the design of an anthropomorphic RRR linkage to achieve the task described in Table 1 with incorporated second order acceleration motion constraints. The design procedure allows the designer to size the RRR chain. The link dimensions of the 3R chain were selected using the finger dimensions of a human subject a1 = 48.93 mm and a2 = 23.74 mm (see Fig. 16 for the notations). Here, the work of Robson, *et al.* [8-11] is followed to introduce relative transformations and obtain a standard set of design equations. As a next step, the design equations are solved. The synthesis solutions for the RRR chain are obtained and Fig. 22 is a planar example of the design of a mechanical finger, incorporating first and second order constraints. The obtained real solution for the RRR finger design is shown in Table 2, where **G1** and **W1** are the MCP and PIP finger joints respectively.

Table 2. Synthesis Solutions for the Location of the MCP and PIP Joints of a Synthesized Anthropomorphic Finger With Velocity and Acceleration Constraints, Compatible With Contact and Curvature Task Requirements

	G_1	W_1
1	$(0,0)$	$(-48.48, -6.60)$
2	$(-139.78, -47.52)$	$(-141.20, -51.68)$
3	*Complex*	*Solution*
4	*Complex*	*Solution*

Thus, for a given set of two task positions, two velocities and one acceleration we can solve the inverse kinematics equations to determine the associated joint parameter vectors of the obtained the RRR chain, shown in Fig. 22.
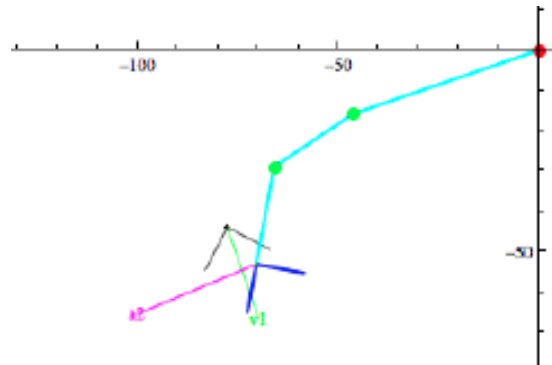
Figure 22. The RRR Chain, Sized According to the Finger Dimensions of the Subject, Performing a Stress Ball Task.

6.2 Spatial Example: Design of Non-Anthropomorphic Fingers for an Anthropomorphic Task

In what follows, a spatial non-anthropomorphic TR finger had been designed, based on a given TRR human finger motion trajectory data. Then the movement of the two fingers has been coordinated for a writing task. The task consists of three positions, two velocities and two accelerations for the fingers. The inverse kinematics of the TRR chain has been solved first and then the TR chain has been synthesized to make sure that both fingers can go smoothly through the specified task.

To determine the seven design parameters of a TR chain, we require seven constraint equations obtained from the task specification (see [9-11] for more details). In order to be able to perform a "writing" task, both mechanical linkages has to have coordinated movement, i.e. one and the same task specifications, follow one and the same trajectory, as well as stay in contact with the pen at all times. The task is defined as positions and higher motion derivatives of the tip of the pen, with acceleration/curvature constraints in the second and third positions (see Table 3).

Table 3. The Task Data With Two Specified Accelerations

Position	$(\theta, \phi, \psi, d_x, d_y, d_z)$	Velocity Data	Acceleration Data
1	$(\frac{\pi}{2}, 0, \frac{\pi}{12}, 5, -1, 5)$	–	–
2	$(\frac{\pi}{2}, \frac{\pi}{6}, 0, 2, 3, 5)$	(2, 5, 1, 2, 3, 5)	(5, 3.5, -1.5, 0.5, 1, 3)
3	$(0, \frac{\pi}{12}, \frac{\pi}{2}, -6, -1, 5)$	(-1, 5, 3, 6, 1, 5)	(1, 3, -3, 5, 1, 5)

Here, the work of Robson, *et al*. [8-11] is followed to introduce relative transformations and obtain a standard set of design equations. As a next step, the design equations are solved. The synthesis solutions for the TR chain are obtained and Fig. 23 is a spatial example of the design of mechanical fingers, incorporating first and second order constraints. The obtained two real solutions for the TR finger design are shown in Table 4, where **B** and **P** are the MCP and PIP finger joints respectively. Solution 2 was chosen for the particular example.
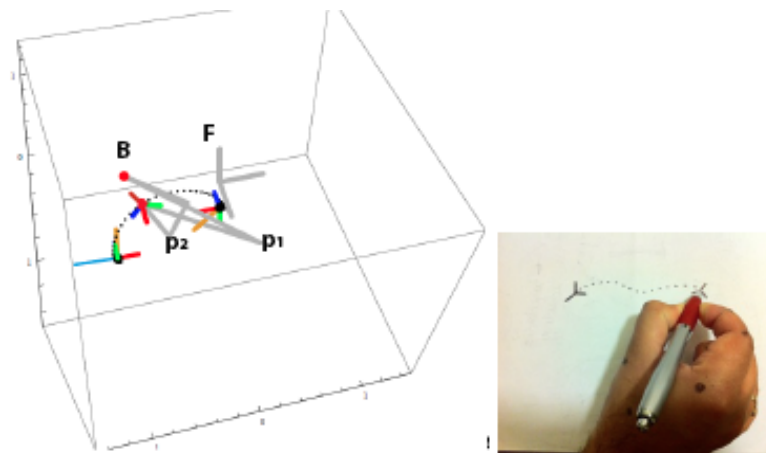
Figure 23. Coordinated Movement of Two Robot Non-Anthropomorphic Fingers: Design of a TR Chain for a Given TRR Motion for Performing a "Writing" Task.

Table 4: The Synthesis Results for the Prescribed Task.

Solution	$\mathbf{B}=(u, v, w)$	$\mathbf{P}=(x, y, z)$
1	(-251.9, -990.2, 1232.2)	(3.1, -6.5, 3.1)
2	(131.0, 353.8, 11.1)	(-2.4, -6.2, -0.2)

Standard trajectory planning techniques are adapted to the constrained movement of the spatial open chain with less than six degrees of freedom. The synthesis equations ensure that the fingertips can achieve the specified task positions, velocities and accelerations. Therefore the goal is to calculate the associated joint angles, joint velocities and joint accelerations. This is done using modifications of the fifth degree polynomial trajectory used to fit position, velocity and acceleration data that is described in Craig [30].

51

7. SUMMARY AND FUTURE WORKS

In this thesis, a preliminary multiple accelerometer equipped prototype deice for capturing accelerations and positions of the fingers is reported. Kinematic Kalman Filter (KKF) is applied in conjunction with the accelerometers for optimal velocity estimation. On comparing the performance of the device with motion capture data, we find that estimation of position and velocity obtained from the device is not significantly different from the motion capture data and its derivatives.

Following this, a preliminary reduced marker protocol for hand motion capture is introduced. This proposes to reduce the number of markers placed on the hand during optical motion capture. By utilizing an inverse kinematics approach based on the geometry of the finger linkages, we are able to show how the complete hand configuration can be reconstructed when employing the reduced marker set for motion capture. During preliminary experiments, the proposed method showed a Root Mean Squared Error (RMSE) of 2° in the estimation of the DIP joint angle for a grasping motion when compared to values obtained from the implementation of a full marker set.

Extending these preliminary results, a second prototype device is formulated in the form of a sensor glove that is furnished with tri-axis accelerometers on the fingertips and optical markers placed in accordance with the reduced marker protocol. To transform the velocity, position and acceleration data obtained from the sensor in the device local frame to a fixed reference frame, the fingers are treated as three degrees of freedom RRR chains and relative position, velocity and acceleration homogeneous

matrices for it are derived. The transformed position, velocity and acceleration data are compared to the Vicon data and its higher derivatives in the fixed frame. We observe that the sensor glove achieves better estimations of acceleration as compared to the preliminary prototype device. Additionally, we find the sensors used in the glove do not suffer from the drawbacks attendant with optical motion capture of hands, namely missing or misidentified marker data.

In future, the use of Kalman Filters for obtaining optimal velocity and position information from the glove will be explored. Additionally, the angular acceleration and velocity of the fingertips will be estimated by applying methods similar to those implemented for the study of linear acceleration and velocity of the fingers. Also, for more accurate velocity and position estimation, the idea of utilizing inertial measurement units is proposed. Furthermore, by utilizing the geometry and the natural constraints of the finger linkage system, the reduced marker protocol will be further refined. It is generally known that there exist certain dependencies between joint angles and their permitted ranges of motion [3] in the natural human hand movement. To our knowledge, there are limited numbers of studies which take into account the natural constraints on the motion of the hand. Future models will incorporate this information to further simplify the calculations. Another vital component to improving the performance of the sensor glove is to accurately estimate and reduce the error due to skin artifact motion.

REFERENCES

[1] Bullock, I. M., Borras, J., and Dollar, A. M., 2012, "Assessing Assumptions in Kinematic Hand Models: A Review," Proc. Biomedical Robotics and Biomechatronics (BioRob), 4th IEEE RAS & EMBS International Conference on, IEEE, pp. 139-146.

[2] Erol, A., Bebis, G., Nicolescu, M., Boyle, R. D., and Twombly, X., 2007, "Vision-Based Hand Pose Estimation: A Review," Computer Vision and Image Understanding, 108(1), pp. 52-73.

[3] Lin, J., Wu, Y., and Huang, T. S., 2000, "Modeling the Constraints of Human Hand Motion," Proc. Human Motion, Proceedings. Workshop on, IEEE, pp. 121-126.

[4] Friedman, J., Flash, T., 2007, "Task-Dependent Selection of Grasp Kinematics and Stiffness in Human Object Manipulation," Cortex, Vol. 43, pp. 444-460.

[5] Aristidou, A., and Lasenby, J., 2010, "Motion Capture With Constrained Inverse Kinematics for Real-Time Hand Tracking," Proc. Communications, Control and Signal Processing (ISCCSP), 4th International Symposium on, IEEE, pp. 1-5.

[6] Cobos, S., Ferre, M., and Aracil, R., 2010, "Simplified Human Hand Models Based on Grasping Analysis," Proc. Intelligent Robots and Systems (IROS), 2010 IEEE/RSJ International Conference on, IEEE, pp. 610-615.

[7] Miyata, N., Kouchi, M., Kurihara, T., and Mochimaru, M., 2004, "Modeling of Human Hand Link Structure From Optical Motion Capture Data," Proc. Intelligent Robots and Systems, (IROS 2004). Proceedings. 2004 IEEE/RSJ International Conference on, IEEE, pp. 2129-2135.

[8] Robson, N. P., 2008, "Geometric Design of Mechanical Linkages for Contact Specifications," Doctor of Philosophy, University of California, Irvine.

[9] Robson, N. P., and McCarthy, J. M., 2007, "Kinematic Synthesis with Contact Direction and Curvature Constraints on the Workpiece," Proc. ASME International Design Engineering Technical Conferences (IDETC/MECH), pp. 581-588.

[10] Robson, N. P., and McCarthy, J. M., 2009, "Applications of the Geometric Design of Mechanical Linkages With Task Acceleration Specifications," ASME.

[11] Robson, N. P., and Tolety, A., 2011, "Geometric Design of Spherical Serial Chains with Curvature Constraints in the Environment," Proc. ASME International Design Engineering Technical Conferences & Computers and Information in Engineering Conference (IDETC/CIE).

[12] Dipietro, L., Sabatini, A. M., and Dario, P., 2003, "Evaluation of an Instrumented Glove for Hand-Movement Acquisition," Journal of Rehabilitation Research and Development, 40(2), pp. 179-190.

[13] Schlattmann, M., Broekelschen, J., and Klein, R., 2009, "Real-Time Bare-Hands-Tracking for 3D Games," Proc. GET, 9, pp. 59-66.

[14] Cerveri, P., De Momi, E., Lopomo, N., Baud-Bovy, G., Barros, R. M. L., and Ferrigno, G., 2007, "Finger Kinematic Modeling and Real-Time Hand Motion Estimation," Annals Of Biomedical Engineering, 35(11), pp. 1989-2002.

[15] Ballan, L., Taneja, A., Gall, J., Van Gool, L., and Pollefeys, M., 2012, "Motion Capture of Hands in Action Using Discriminative Salient Points," Proc. European Conference on Computer Vision (ECCV), pp. 640-653.

[16] Chang, L. Y., Pollard, N. S., Mitchell, T. M., and Xing, E. P., 2007, "Feature Selection for Grasp Recognition From Optical Markers," Proc. Intelligent Robots and Systems, IROS 2007. IEEE/RSJ International Conference on, IEEE, pp. 2944-2950.

[17] Simone, L. K., Sundarrajan, N., Luo, X., Jia, Y., & Kamper, D. G. , 2007, "A Low Cost Instrumented Glove for Extended Monitoring and Functional Hand Assessment", Journal of neuroscience methods, 160(2), 335-348.

[18] Quam, D. L. , 1990, "Gesture Recognition With a DataGlove", Aerospace and Electronics Conference, 1990. NAECON 1990., Proceedings of the IEEE 1990 National (pp. 755-760). IEEE.

[19] Quam, D., Williams, G., Agnew, J., and Browne, P. , 1989, "An Experimental Determination of Human Hand Accuracy With a DataGlove", Proceedings of the Human Factors Society 33rd Annual Meeting, pp. 315-319.

[20] Kessler, G. D., Hodges, L. F., & Eng'neewng, N. W. , 1995, "Evaluation of the Cyberglove as a Whole-Hand Input Device", ACM's transactions on computer-human interaction, 2(4), 263-283.

[21] Vecchi, F., Micera, S., Zaccone, F., Carrozza, M. C., Sabatini, A. M., & Dario, P., 2001, "A Sensorized Glove for Applications in Biomechanics and Motor Control", 6th IFESS Conf.

[22] Perng, J. K., Fisher, B., Hollar, S., & Pister, K. S., 1999, "Acceleration Sensing Glove (ASG)", Wearable Computers, 1999. Digest of Papers. The Third International Symposium on (pp. 178-180). IEEE.

[23] Gülke, J., Gulkin, D., Wachter, N., Knöferl, M., Bartl, C., & Mentzel, M., 2012, "Dynamic Aspects During the Cylinder Grip—Flexion Sequence of the Finger Joints Analyzed Using a Sensor Glove", Journal of Hand Surgery (European Volume).

[24] Schiessl, S. K. J., 2004, " Acoustic Chase: Designing an Interactive Audio Environment to Stimulate Human Body Movement", Doctoral dissertation, Massachusetts Institute of Technology.

[25] Sturman, D. J., and Zeltzer, D., 1994, "A Survey of Glove-Based Input," Computer Graphics and Applications, IEEE, 14(1), pp. 30-39.

[26] Jeon, S., 2010,"State Estimation Based on Kinematic Models Considering Characteristics of Sensors," Proc. American Control Conference (ACC), IEEE, pp. 640-645.

[27] Thies, S. B., Tresadern, P., Kenney, L., Howard, D., Goulermas, J. Y., Smith, C., & Rigby, J., 2007, "Comparison of Linear Accelerations From Three Measurement Systems During "Reach & Grasp",". Medical engineering & physics,29(9), 967-972.

[28] Aravind, V. R., 2004, "VICON Volume Visualization," MS, University of Hull.

[29] Lisa, S., Derek, K., "Design Considerations for a Wearable Monitor to Measure Finger Posture", Journal of NeuroEngineering and Rehabilitation, 2.

[30] Craig, J. J., 2004, "Introduction to Robotics, Mechanics and Control," Prentice Hall.

[31] McCarthy, J. M., & Soh, G. S., 2010, "Geometric Design of Linkages," (Vol. 11), Springer.